

PREDICTING PARTICLE CRITICAL SUPERSATURATION FROM HYGROSCOPIC
GROWTH MEASUREMENTS IN THE HUMIDIFIED TDMA.
PART I: THEORY AND SENSITIVITY STUDIES

F. J. Brechtel and S. M. Kreidenweis*
Atmospheric Sciences Division
Environmental Sciences Department
Brookhaven National Laboratory
Upton, NY 11973-5000

July 2000

Published in
Journal of the Atmospheric Sciences
[vol. 57, 1854-1871, 2000]

* Corresponding author: Dept. of Atmospheric Science, Colorado State University, Fort Collins, CO.

By acceptance of this article, the publisher and/or recipient acknowledges the U.S. Government's right to retain a nonexclusive, royalty-free license in and to any copyright covering this paper.

Research by BNL investigators was performed under the auspices of the U.S. Department of Energy under Contract No. DE-AC02-98CH10886.

Predicting Particle Critical Supersaturation from Hygroscopic Growth Measurements in the Humidified TDMA. Part I: Theory and Sensitivity Studies

FRED J. BRECHTEL* AND SONIA M. KREIDENWEIS

Department of Atmospheric Science, Colorado State University, Fort Collins, Colorado

(Manuscript received 21 October 1998, in final form 22 July 1999)

ABSTRACT

A method is described to estimate the critical supersaturation of quasi-monodisperse, dry particles using measurements of hygroscopic growth at relative humidities below 100%. Köhler theory is used to derive two chemical composition-dependent parameters, with appropriate accounting for solution effects through a simplified model of the osmotic coefficient. The two unknown chemical parameters are determined by fitting the Köhler model to data obtained from humidified tandem differential mobility analyzer (HTDMA) measurements, and used to calculate the critical supersaturation for a given dry particle size. In this work the theory and methodology are presented, and sensitivity studies are performed, with respect to assumptions made and uncertainties in key input parameters to the Köhler model.

Results show that for particle diameters of 40 and 100 nm, the average error between critical supersaturations derived using the proposed method and theoretical values is -7.5% ($1\sigma = 10\%$, $n = 16$). This error is similar to experimental uncertainties in critical supersaturations determined from laboratory studies on particles of known chemical composition (-0.6% , $1\sigma = 11\%$, $n = 16$).

1. Introduction

A recent report by the Intergovernmental Panel on Climate Change (IPCC) indicates that current estimates of the uncertainty in predictions of the indirect effect of aerosols on climate are at least twice as large as the total direct effect of CO_2 , and of opposite sign (IPCC 1995). The so-called indirect effect is the ability of particulate matter to alter climate by acting as cloud condensation nuclei (CCN) and thereby altering cloud radiative properties. In order to better understand the roles played by various sources of ambient particles in determining the CCN population, experimental techniques are needed to link particle size and chemical composition to CCN activity.

A key parameter in the relationship among particle size, chemical composition, and CCN activity is the critical supersaturation, S_{crit} , the water supersaturation necessary to activate a cloud condensation nucleus and form a cloud droplet. At any given size, particles having different chemical compositions can exhibit different

values of S_{crit} . Knowledge of how the critical supersaturation varies among similar-sized particles and across the size spectrum can reveal the size ranges of particles that would form cloud droplets in different cloud-forming regimes (Fitzgerald et al. 1982; Hudson and Da 1996). Conventional CCN spectrometers typically measure the integral number of particles of all sizes that are activated at a given supersaturation.

In Part I of this work, a technique is proposed to directly relate particle size and chemical composition to its critical supersaturation by performing a mathematical regression of a modified form of the Köhler equation to hygroscopic growth measurements at relative humidities (RHs) below 100%. A modified Köhler theory is required in this application in order to constrain the solutions to realistic values and to minimize the number of chemical composition-dependent unknowns that must be determined by the mathematical regression. Numerical sensitivity studies are performed to test the assumptions made in the modified theory and demonstrate the accuracy of predictions of the critical supersaturation for particle diameters of 40 and 100 nm. The 40–100-nm size range is important relative to CCN activity since a large fraction of the CCN number concentration at S_{crit} values around 0.5% occurs in this size range (Covert et al. 1998; Hallberg et al. 1994). We note that the current version of the modified Köhler theory does not explicitly account for the effects of undissolved material, soluble gases, and surface-active compounds on S_{crit}

* Current affiliation: Environmental Chemistry Division, Brookhaven National Laboratory, Upton, New York.

Corresponding author address: Sonia M. Kreidenweis, Dept. of Atmospheric Science, Colorado State University, Fort Collins, CO 80523.

E-mail: soniak@aerosol.atmos.colostate.edu

TABLE 1. Summary of previous HTDMA studies in both clean and influenced maritime (CM and IM) and continental conditions (CC and IC). "All" designates all air mass conditions, "I" = internally mixed, "E" = externally mixed chemical composition and "—" implies not observed. A less hygroscopic particle subpopulation, if observed, is designated as "less hygro," while a more hygroscopic population is designated as "more hygro." Simultaneous chemical composition measurements designated by "Y" in "chem. meas." column. The size ranges of particle samples depend on the individual study, but the 30–200-nm size range is representative of the sizes sampled.

Study	Location (cond.)	Study RH (%)	$D_{\text{drop}}/D_{p,\text{sol}}$ Less hygro	$D_{\text{drop}}/D_{p,\text{sol}}$ More hygro	Inferred mixture	Chem. meas.
a	IC	80	—	1.2–1.8	I	N
b	IC	90	1.0	1.12–1.49	E	Y
c	IC	90	1.07	1.38–1.44	E	Y
d	CC, IC	85	1.15	1.36–1.51	E, I	Y
e	CC, IC	90	1.05	1.44–1.48	E	Y
f	IC	—	—	—	E	N
g	IC	85	1.1	1.44	E	Y
h	IC, CC	85	1.02–1.11	1.34–1.37	E, I	Y
i	CC, IC	85	1.15	1.43	E, I	Y
j	IC	79	1.02	1.3	E, I	N
k	CM, IM	50, 85	1.1	1.4	E, I	Y
l	All	90	1.1	1.5	E, I	Y
m	IC	90	1.0	1.4	E	Y
n	Lab	80–97	1.0	0.94	I	Y

a: Sekigawa (1983); insoluble fraction varies with D_p .

b: McMurry and Stolzenburg (1989); Los Angeles (SCAQs); larger D_p more hygroscopic (1.33 \times).

c: Covert and Heintzenberg (1984); carbon in less hygroscopic fraction.

d: Zhang et al. (1993); Grand Canyon winter 1990 (NGS and SCAQS); insoluble inclusions; hygroscopicity was a function of [ions]/[carbon].

e: Covert and Heintzenberg (1993); sulfur and carbon in more hygroscopic fraction.

f: Juozaitis et al. (1993); high soot; observed hydrophobic size distribution, 60% hydrophobic fraction at 0.02 μm , 15% at 0.05 μm , 4% at 0.45 μm .

g: Svenningsson et al. (1992); potential large organic influence; hygroscopic growth not $f(D_p)$, nonhygroscopic and hygroscopic fractions equal.

h: Svenningsson et al. (1994); 50% of CN concentration nonhygroscopic.

i: Pitchford and McMurry (1994); NGS and SCAQS; 85% of CN volume in nonhygroscopic fraction nonsoluble.

j: Liu et al. (1978); Minneapolis, MN; focused on H_2SO_4 .

k: Berg et al. (1998); ACE-1 study; *Discoverer*.

l: Covert et al. (1998); ACE-1 study; Cape Grim.

m: McMurry et al. (1996); less hygro = C chains, more hygro = liquid drops with S and some C.

n: Weingartner et al. (1997); combustion particles; particles shrink with increasing RH up to 95% RH.

(Laaksonen et al. 1998; Schulmann et al. 1996). In Part II (Brechtel and Kreidenweis 2000) results from laboratory studies performed to test the method are presented.

2. Previous work

The hygroscopicity of submicrometer particles can be investigated as a function of size using the humidified tandem differential mobility analyzer technique (HTDMA; Rader and McMurry 1986). In the HTDMA, dry (RH < 10%), quasi-monodisperse particles are selected from a polydisperse size distribution using a differential mobility analyzer (DMA). The DMA selects particles based upon their electrical mobility, which is directly proportional to the number of elementary electrical charges carried by the particle and inversely proportional to its size. The monodisperse particles are exposed to a controlled humidity environment before passing through a second DMA. If the particles take up water, they will grow in size and exhibit a lower electrical mobility in the second DMA. A condensation par-

ticle counter (CPC) is used to count the particles exiting the second DMA. By observing the electrical mobility where the CPC measures the maximum number of particles, the size of the wetted particles can be determined, and the water content can be derived from the difference between the wet and dry sizes. By controlling the humidities before and within the second DMA at several different values, the growth as a function of relative humidity may be determined for each input, dry monodisperse particle population.

There have been several previous studies of particle hygroscopic growth using the HTDMA technique, but only a few of these also involved a determination of S_{crit} . A summary of several HTDMA studies is provided in Table 1. In their HTDMA measurements on ambient particles in the polluted Po Valley of Italy, Svenningsson et al. (1992) determined that the chemical composition of individual particles was just as important as size in determining whether they are CCN. Other HTDMA studies (Covert and Heintzenberg 1993; McMurry and Stolzenburg 1989) demonstrated that the chemical composition of ambient particles was heterogeneous with

respect to particle size. Zhang et al. (1993) and Pitchford and McMurry (1994) inferred that the ambient particle chemical composition was heterogeneous over a narrow size range, based on observations of more than one hygroscopic mode at a single particle size during both anthropogenically influenced and more remote continental conditions. Covert et al. (1998) found that even in remote marine regions, the CCN activity could best be determined from hygroscopic growth measurements during periods characterized by relatively simple particle chemical compositions.

There have been only a few studies where S_{crit} was derived using HTDMA measurements. Svenningsson et al. (1992) and Covert et al. (1998) used simultaneous composition measurements from impactor samples to determine the chemical composition of the hygroscopic fraction of ambient particulate matter. Weingartner et al. (1997) performed HTDMA measurements on combustion particles to predict their critical supersaturation. No simultaneous CCN measurements were conducted, although derived values of S_{crit} compared favorably with historical measurements of the CCN activity of combustion particles.

Recently, organics have been recognized as playing a role toward determining particle hygroscopicity (Saxena et al. 1995; Saxena and Hildemann 1996). Cruz and Pandis (1997) measured the critical supersaturations necessary to activate monodisperse particles composed of organic acids, compounds that have been found in ambient particles (Rogge et al. 1993). Cruz and Pandis (1997) demonstrated that Köhler theory could be used to predict S_{crit} for less soluble organics within the experimental uncertainties of their method.

In this work, a methodology is proposed to extend estimates of hygroscopic growth to RHs above 100% by incorporating a thermodynamic model of water activity with correct limiting behavior. The approach enables S_{crit} to be determined from a series of hygroscopic growth measurements made at relative humidities less than 100%. The applicability of the method to particles composed of single and mixed solutes is examined.

3. Theoretical approach

Droplets formed on soluble particles at relative humidities between 80% and 92%, a typical range for HTDMA studies, experience molalities between about 1 and 6 molal. At these relatively high concentrations, inter-ion interactions modify the vapor pressure lowering over the droplet surface as described by Raoult's law. The Köhler equation, which describes the equilibrium water vapor pressure over a droplet formed on a soluble nucleus, must include an appropriate model for the change in water activity with solution molality.

The Köhler equation for a droplet containing water-soluble material may be written (Seinfeld 1986)

$$\text{RH} = 100a_w \exp\left[\frac{4\bar{\sigma}_{\text{drop}}\bar{v}_l}{RTD_{\text{drop}}}\right], \quad (1)$$

where RH is in percent, $\bar{\sigma}_{\text{drop}}$ is the droplet surface tension, \bar{v}_l is the partial molar volume of water in solution, R is the universal gas constant, T is the droplet temperature, D_{drop} is the droplet diameter, and a_w is the water activity of the solution. Here $\bar{\sigma}_{\text{drop}}$, \bar{v}_l , and a_w are functions of temperature and solution composition. The exponential term on the right-hand side of Eq. (1) is generally referred to as the Kelvin, or curvature, term.

For aqueous solutions of ionic compounds, a_w may be written (Robinson and Stokes 1959)

$$a_w = \exp\left[\frac{-M_w\nu\Phi m}{1000}\right], \quad (2)$$

where M_w is the molecular weight of pure water, ν is the total number of ions produced by the dissociation of one molecule of solute, Φ is the practical osmotic coefficient of the solution, and m is the solution molality. For an infinitely dilute solution, $a_w = 1$. The term $\ln(a_w)$ is often referred to as the solute or Raoult term, where the often used van't Hoff factor has been replaced by the more exact form represented by the product $\nu\Phi$. The common assumption that the solution is dilute ($\Phi = 1$; Pruppacher and Klett 1997), appropriate for cloud droplets, is not valid under most HTDMA measurement conditions. Our calculations show that even at the critical size, the assumption that $\Phi = 1$ corresponds to errors in predicted values of S_{crit} of 20% for a dry 10-nm-diameter particle composed of ammonium sulfate and 5% for a 300-nm dry diameter and the same composition (Brechtel 1998). Therefore, we retain the variation of the osmotic coefficient with solution composition.

a. Reference Köhler model

In this section we develop the full, or reference, Köhler model in terms of parameters to be determined from HTDMA studies. Then we develop the modified form of the Köhler equation used in the HTDMA data regression procedure and show the sensitivities of the predicted RH and S_{crit} values to the various assumptions.

The droplet surface tension is corrected for temperature and solute effects using the relationship proposed by Hänel (1976)

$$\bar{\sigma}_{\text{drop}} = \sigma_o(T_o) + a(T_o - T) + bm, \quad (3)$$

where $\sigma_o(T_o)$ is the surface tension of pure water at $T_o = 273.15$ K (0.0756 N m⁻¹), a is a coefficient to account for the temperature dependence of the droplet surface tension [$a = 1.53 \times 10^{-4}$ N (m K)⁻¹], b is a composition-dependent factor listed in Table 2, and m is the solution molality. Values of $\bar{\sigma}_{\text{drop}}$ as a function of solute mass fraction are shown in Fig. 1 for most of the solutes investigated in this work.

The molality m is defined as the number of moles of

TABLE 2. Values of ρ_s , M_s , β_0 , surface tension 'b' parameter, deliquescence RH, and crystallization RH for solute chemical compositions examined in this work. Values for mixed composition solutes assume an equimolar mixture of the two salts.

Solute	Ratio Cation/Anion	ρ_s^a kg m ⁻³	M_s^a g mol ⁻¹	β_0^b	$\frac{N \text{ mol}_w}{\text{mkg}_{\text{sol}}} \times 10^{-3}$ b^c	RHdel ^d %	RHcrys ^d %
NaCl	1:1	2165	58.44	0.1082	1.64	75.3	45–48
(NH ₄) ₂ SO ₄	2:1	1769	132.1	0.04763	2.17	80	37–40
NH ₄ HSO ₄	1:1	1780	115.1	0.04494	2.3	40	0.05–22
H ₂ SO ₄	2:1	1841	98.01	-0.0933	0.67		
NH ₄ NO ₃	1:1	1725	80.04	-0.0154	2.2	62	
(NH ₄) ₂ H(SO ₄) ₂	4:2	1830	247.0	0.0463	2.2	69	35–44
(NH ₄) ₂ SO ₄ -NaCl	3:2	1874	95.30	0.078	1.91		
(NH ₄) ₂ SO ₄ -NH ₄ NO ₃	3:2	1752	106.1	0.016	2.185		
NaCl-NH ₄ NO ₃	2:2	1887	69.24	0.0464	1.6		
NaCl-Na ₂ SO ₄	3:2	2506	100.2	0.048	2.05	84 ^e	53 ^e

^a Weast (1988).

^b Pitzer and Mayorga (1973).

^c Chen (1994).

^d Tang and Munkelwitz (1994).

^e Tang (1997).

solute per kilogram of water and may be written for the droplet solution as

$$m = \frac{1000m_s}{M_s m_w} = \frac{1000x_s}{M_s(1-x_s)}, \quad (4)$$

where m_s and m_w are the masses of solute and water in the droplet, respectively; M_s is the molecular weight of the solute; and x_s is the mass fraction of solute in solution, defined by

$$x_s = \frac{m_s}{m_s + m_w} = \frac{\rho_s D_{p,\text{sol}}^3}{\rho_{\text{drop}} D_{\text{drop}}^3}, \quad (5)$$

where ρ_s and ρ_{drop} are the densities of the solute and solution, respectively; and $D_{p,\text{sol}}$ and D_{drop} are the dry particle and droplet size, respectively. Equation (5) assumes that the dry particle is completely dissolved in solution.

The partial molar volume of water in the droplet solution may be written (Atkins 1994)

$$\bar{v}_l = \frac{M_w}{\rho_{\text{drop}}} \left[1 + \frac{x_s}{\rho_{\text{drop}}} \frac{d\rho_{\text{drop}}}{dx_s} \right], \quad (6)$$

where $d\rho_{\text{drop}}/dx_s$ is the change in solution density with mass fraction of solute and reflects the fact that intermolecular forces in solution change with changing solute mass fraction. The ρ_{drop} and $d\rho_{\text{drop}}/dx_s$ may be calculated for droplet solutions containing the solutes studied here from polynomials of ρ_{drop} as functions of x_s from Tang and Munkelwitz (1994), Tang et al. (1981), and Tang (1997). Values of \bar{v}_l as a function of solute mass fraction are shown in Fig. 1.

The most difficult part of predicting S_{crit} using results from HTDMA studies is dealing with Φ . No purely theoretical model of the osmotic coefficient currently exists. Only semiempirical models based on theoretical considerations are available for Φ (Pitzer and Mayorga

1973; Pitzer 1973; Kim et al. 1993; Clegg and Pitzer 1992). Guidance in choosing a parameterization for Φ comes from the model of Pitzer and Mayorga (1973), which was capable of reproducing the variation of Φ with molality for solutions containing a single solute for over two hundred 1:1, 1:2, and 2:1 solutes. They proposed the following functional form for Φ for electrolyte solutions:

$$\Phi = 1 - |z_1 z_2| \left[A_\phi \frac{\sqrt{I}}{1 + b_{\text{pit}} \sqrt{I}} \right] + m \frac{2\nu_1 \nu_2}{\nu} [\beta_0 + \beta_1 e^{-\alpha \sqrt{I}}] + m^2 \frac{2(\nu_1 \nu_2)^{3/2}}{\nu} C_\phi. \quad (7)$$

In the above equation, α and b_{pit} are 2 and 1.2 at 298 K, respectively, for all of the solutes examined; z_1 and z_2 are the respective charges on the ions in electronic units; ν_1 and ν_2 are the number of molecules of ions of species 1 and 2, respectively, produced by the dissociation of one molecule of solute; ν is $\nu_1 + \nu_2$; and I is the ionic strength of the solution, $\frac{1}{2} \sum m_i z_i^2$, where m_i is the molality of species i and the sum is carried out over the total number of ionic species present. We note that Eq. (7) is explicitly written for solutes that dissociate into two ions in solution. The relation for Φ for solutions with more ions requires additional terms to account for the additional ion-pair interactions in solution. The coefficients β_0 , β_1 , and C_ϕ depend on the chemical composition of the solute and are tabulated by Pitzer and Mayorga (1973) and Kim et al. (1993). The Debye-Hückel coefficient for the osmotic function A_ϕ is calculated as a function of temperature (T) for temperatures between 10° and 50°C using the following polynomial fit to data from Pitzer (1979)

$$A_\phi = 6.97714 \times 10^{-4} T + 0.3741. \quad (8)$$

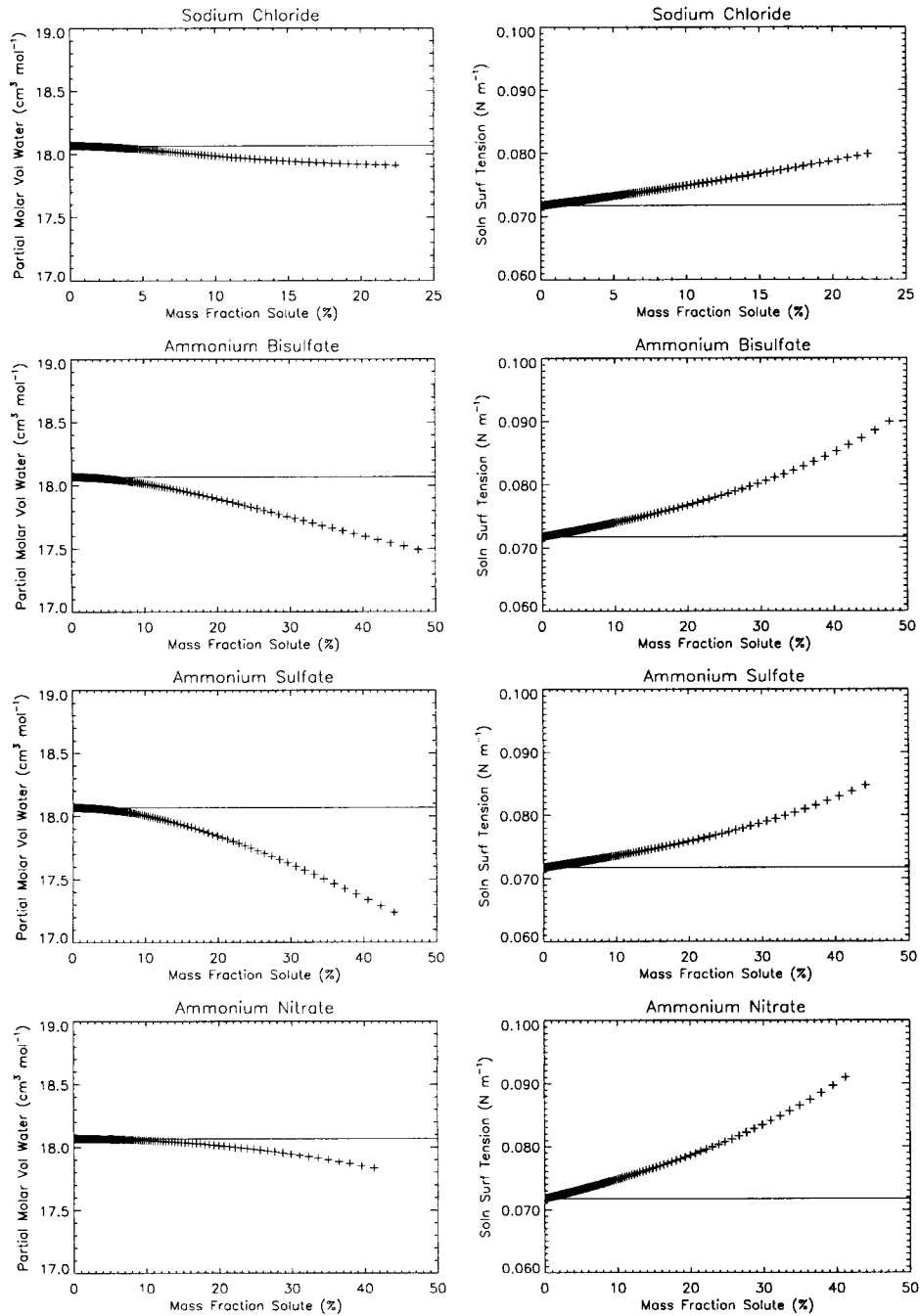


FIG. 1. Partial molar volume of water and solution surface tension values vs solute mass fraction for solute chemical compositions examined in this work. The mass fraction ranges correspond to HTDMA relative humidities between 80% and 95%. The solid horizontal lines represent the respective values for pure water.

The value of A_ϕ is 0.392 for water at 25°C. Equation (7) will be referred to as the “full Pitzer” model of Φ . In the full Pitzer model of Φ , the term involving A_ϕ models the long-range forces through which ions in solution interact and determines the value of Φ when the solution becomes very dilute. As m approaches zero the

ionic strength of the solution also approaches zero, and Φ approaches unity, the thermodynamic limit. The terms involving m model the interaction forces between ions and are important in more concentrated solutions.

Substituting the above relations for $\bar{\sigma}_{\text{drop}}$, \bar{v}_l , and m into the Köhler equation Eq. (1) and Eq. (2) we find

TABLE 3. Values of critical diameters (nm), supersaturations (%), and osmotic coefficients at the critical supersaturation for chemical compositions studied in this work. Results are reported for indicated dry particle sizes and assumed temperature of 29.5°C.

	$D_{p,sol}$ (nm)			
	40	70	100	200
Sodium Chloride NaCl				
D_{crit}	321	748	1285	3668
S_{crit}	0.475	0.203	0.119	0.042
Φ_{crit}	0.937	0.951	0.960	0.974
Amm. Bisulf. NH_4HSO_4				
D_{crit}	210	484	829	2364
S_{crit}	0.730	0.314	0.184	0.064
Φ_{crit}	0.925	0.942	0.952	0.968
Amm. Sulf. $(\text{NH}_4)_2\text{SO}_4$				
D_{crit}	210	504	879	2575
S_{crit}	0.705	0.295	0.170	0.058
Φ_{crit}	0.778	0.832	0.863	0.911
Sulfuric Acid H_2SO_4				
D_{crit}	239	590	1039	1818
S_{crit}	0.603	0.249	0.143	0.012
Φ_{crit}	0.752	0.826	0.863	0.840
Amm. Nitrate NH_4NO_3				
D_{crit}	255	598	1029	2944
S_{crit}	0.534	0.228	0.133	0.046
Φ_{crit}	0.922	0.943	0.954	0.971
Sodium Chloride–Sodium Sulf. $\text{NaCl–Na}_2\text{SO}_4$				
D_{crit}	278	685	1185	3407
S_{crit}	0.447	0.190	0.110	0.038
Φ_{crit}	0.858	0.895	0.914	0.943
Sodium Chloride–Amm. Sulf. $\text{NaCl–}(\text{NH}_4)_2\text{SO}_4$				
D_{crit}	166	421	730	2109
S_{crit}	0.709	0.304	0.176	0.061
Φ_{crit}	0.823	0.869	0.891	0.928
Sodium Chloride–Amm. Nit. $\text{NaCl–NH}_4\text{NO}_3$				
D_{crit}	187	467	804	2288
S_{crit}	0.644	0.278	0.162	0.057
Φ_{crit}	0.916	0.939	0.950	0.968
Amm. Sulf.–Amm. Nit. $(\text{NH}_4)_2\text{SO}_4\text{–NH}_4\text{NO}_3$				
D_{crit}	147	380	662	1915
S_{crit}	0.780	0.334	0.193	0.066
Φ_{crit}	0.799	0.855	0.881	0.922

$$\text{RH} = 100 \exp \left[\frac{4 \left[\sigma_0 + b \frac{1000x_s}{M_s(1-x_s)} \right] M_w}{\rho_{\text{drop}} RT D_{\text{drop}}} \left[1 + \frac{x_s}{\rho_{\text{drop}}} \frac{d\rho_{\text{drop}}}{dx_s} \right] \right] \times \exp \left[\frac{-M_w x_s \nu \Phi}{M_s(1-x_s)} \right], \quad (9)$$

where the temperature dependence of the surface tension has been absorbed into the σ_0 term. We have applied Eq. (9) to a variety of compounds selected as illustrative examples, as shown in Table 3. Parameters for Pitzer's model of Φ were taken from Pitzer and Mayorga (1973). All other property data were obtained from Weast

(1988). Equation (9) will be referred to as the reference Köhler model.

b. Evaluation of mixture properties

Equation (9) has been written for a single solute. In order to study the hygroscopic growth of particles containing two salts, expressions are required to calculate the chemical composition-dependent parameters for internally mixed solutes. Designating the mole fractions of solute "a" and solute "b" as f_a and f_b , respectively, the molecular weight of the mixed solute particle is

$$M_s = f_a M_{s,a} + f_b M_{s,b}, \quad (10)$$

where $M_{s,a}$ is the molecular weight of solute a and $M_{s,b}$ is the molecular weight of solute b. The mass fractions of the two solutes can be determined from

$$x_{s,a} = \frac{f_a M_{s,a}}{M_s}, \quad \text{and similarly} \quad (11)$$

$$x_{s,b} = \frac{f_b M_{s,b}}{M_s}. \quad (12)$$

Using the calculated mass fractions, the solute density ρ_s may be determined from

$$\rho_s = \frac{1}{\frac{x_{s,a}}{\rho_{s,a}} + \frac{x_{s,b}}{\rho_{s,b}}}, \quad (13)$$

where $\rho_{s,a}$ is the density of pure solute a and $\rho_{s,b}$ is the density of pure solute b. Furthermore, the mole fraction weighted number of ions produced when one molecule of the mixed solute dissolves in solution may be calculated from

$$\nu = f_a(\nu_{1,a} + \nu_{2,a}) + f_b(\nu_{1,b} + \nu_{2,b}), \quad (14)$$

where $\nu_{1,a}$ and $\nu_{2,a}$ are the number of anions and cations, respectively, resulting from the dissociation of one molecule of solute a and $\nu_{1,b}$ and $\nu_{2,b}$ are the respective values for solute b. Assuming volume additivity, the droplet solution density may be calculated using the expression from Tang (1997),

$$\rho_{\text{drop}} = \frac{1}{\frac{x_{s,a}}{\rho_{\text{drop},a}} + \frac{x_{s,b}}{\rho_{\text{drop},b}}}, \quad (15)$$

where $\rho_{\text{drop},a}$ and $\rho_{\text{drop},b}$ are the corresponding solution densities of the binary solutions evaluated at the total mass fraction of solute in solution (x_s). For internally mixed solutes, the term involving the derivative of ρ_{drop} with respect to the solute mass fraction in Eq. (9) is evaluated by differentiating Eq. (15) with respect to x_s , where the dependence of ρ_{drop} on x_s is through $\rho_{\text{drop},a}$ and $\rho_{\text{drop},b}$ in Eq. (15). The surface tension of the mixed salt solution is determined from (Chen 1994)

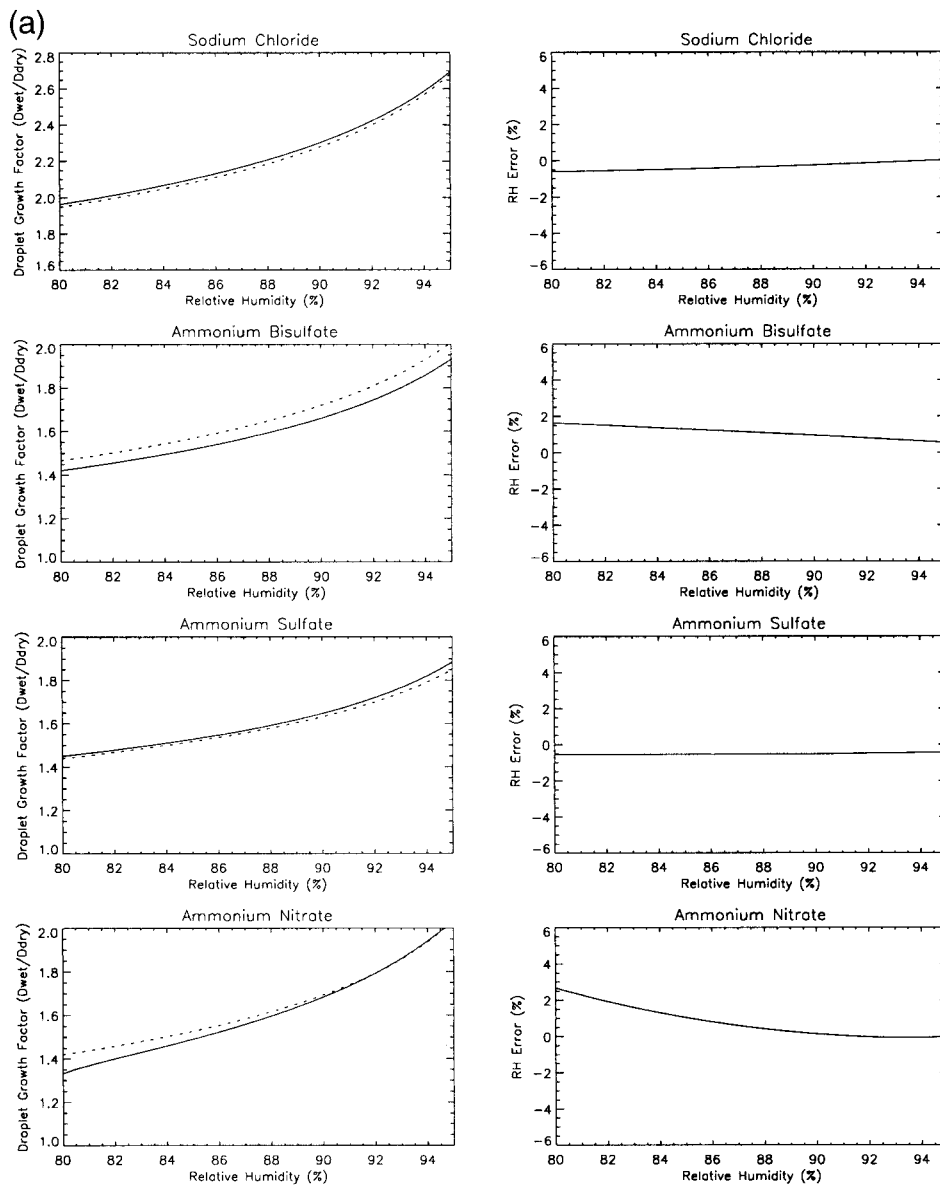


FIG. 2. (a) Comparison of RHs predicted from results of Tang and Munkelwitz (1994) (dotted lines) and reference Köhler model (solid lines) for particles composed of single solutes.

$$\sigma = \sigma_o + b_a m_a + b_b m_b, \quad (16)$$

where b_a and b_b are listed in Table 2, and m_a and m_b are the molalities of solutes a and b in the ternary solution, respectively. Following Pruppacher and Klett (1997), we use a molality weighting approach to evaluate the osmotic coefficient of the solution containing two solutes,

$$\Phi_{s,\text{mix}} = \frac{m_a(\nu_{1,a} + \nu_{2,a})\Phi_{s,a} + m_b(\nu_{1,b} + \nu_{2,b})\Phi_{s,b}}{m_a(\nu_{1,a} + \nu_{2,a}) + m_b(\nu_{1,b} + \nu_{2,b})}, \quad (17)$$

where $\Phi_{s,a}$ is the osmotic coefficient for a binary solution of solute a and water, and $\Phi_{s,b}$ is the osmotic coefficient for a binary solution of solute b and water. The above

expressions were used in Eq. (9) to calculate the equilibrium RH over droplets consisting of ternary solutions of water and the mixed solutes listed in Table 2. As described below, the results were successfully validated against data reported by Tang (1997).

4. Reference model calculations

Correct values of RH in equilibrium with the vapor pressure over a solution having a given mass fraction of solute are required to compare subsequent values of RH predicted from modified versions of the Köhler equation. For calculations involving particles containing single solutes, the mass fraction, x_s , of solute in a drop

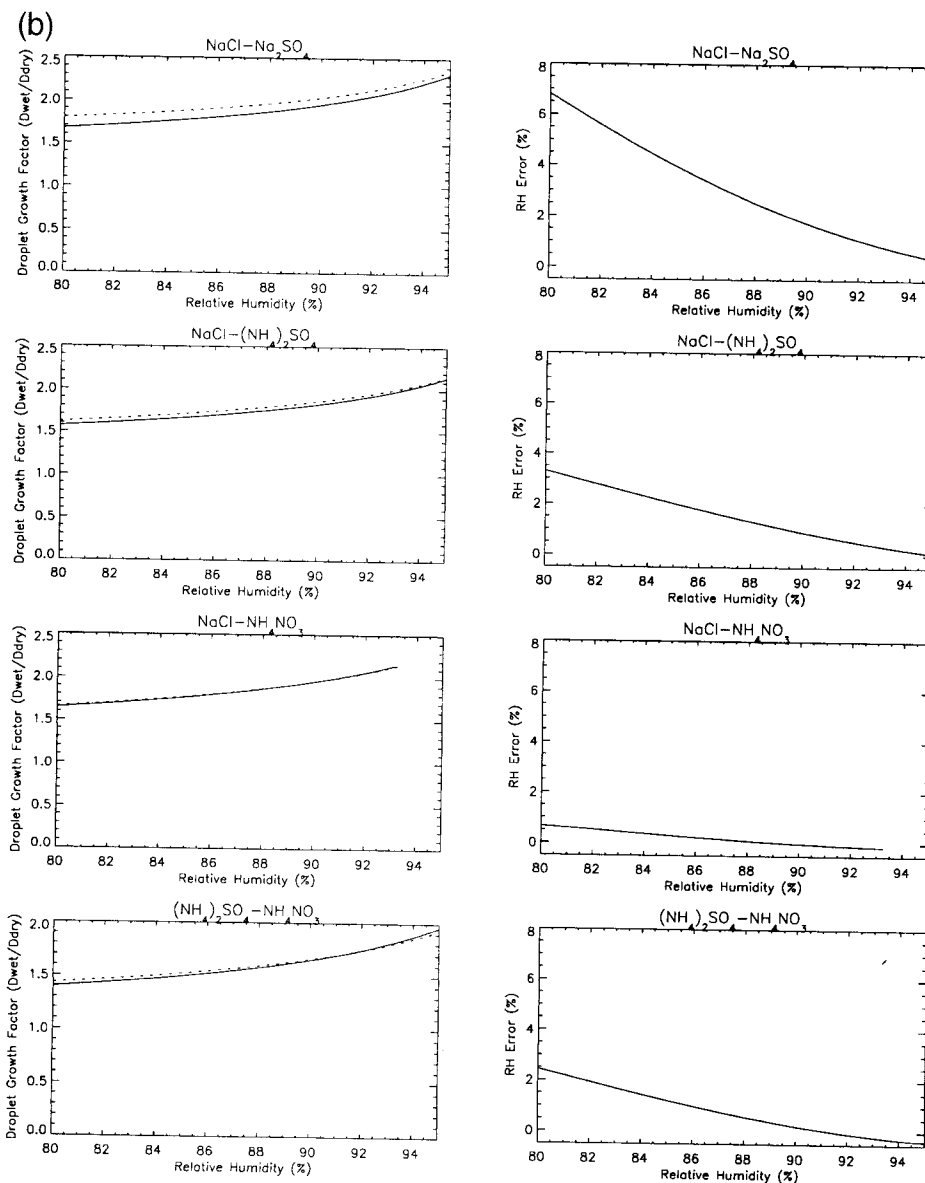


FIG. 2. (Continued) (b). Comparison of RHs predicted from ZSR-Tang relation (dotted lines) and reference Köhler model (solid lines) for internally mixed, equimolar solutes.

of diameter D_{drop} formed on a dry particle of size $D_{p,\text{sol}}$ was found by iteratively solving

$$\rho_{\text{drop}}(x_s)x_s D_{\text{drop}}^3 - \rho_s D_{p,\text{sol}}^3 = 0, \quad (18)$$

where $\rho_{\text{drop}}(x_s)$ designates the polynomial fit of solution density to solute mass fraction. The molality corresponding to this mass fraction was used to compute $\bar{\sigma}_{\text{drop}}$ [Eq. (3)] and Φ [Eq. (7)]. The equilibrium RH for the particular $D_{p,\text{sol}}$ and D_{drop} was then determined using the reference Köhler model [Eq. (9)] and is referred to in this work as the “reference value” of RH. To examine the accuracy of the expression used to compute Φ , the same value of x_s used in the reference Köhler model was also used in the polynomial fits for a_w compiled by

Tang and Munkelwitz (1994), and the corresponding RH calculated using Eq. (1). The values of a_w from the polynomial fits are generally regarded as more accurate than values from other techniques (Kim et al. 1993). Values of D_{crit} , S_{crit} , and Φ at S_{crit} (Φ_{crit}) calculated using the reference Köhler model are shown in Table 3 for various dry particle sizes and compositions. Values of RH calculated using the reference Köhler model (solid lines) are compared with values determined using the results of Tang and Munkelwitz (1994) (dotted lines) in Fig. 2a for binary solutions in order to validate the results from the reference model. Also shown is the percent error between the values of RH predicted by the two methods. The same droplet diameter was used in

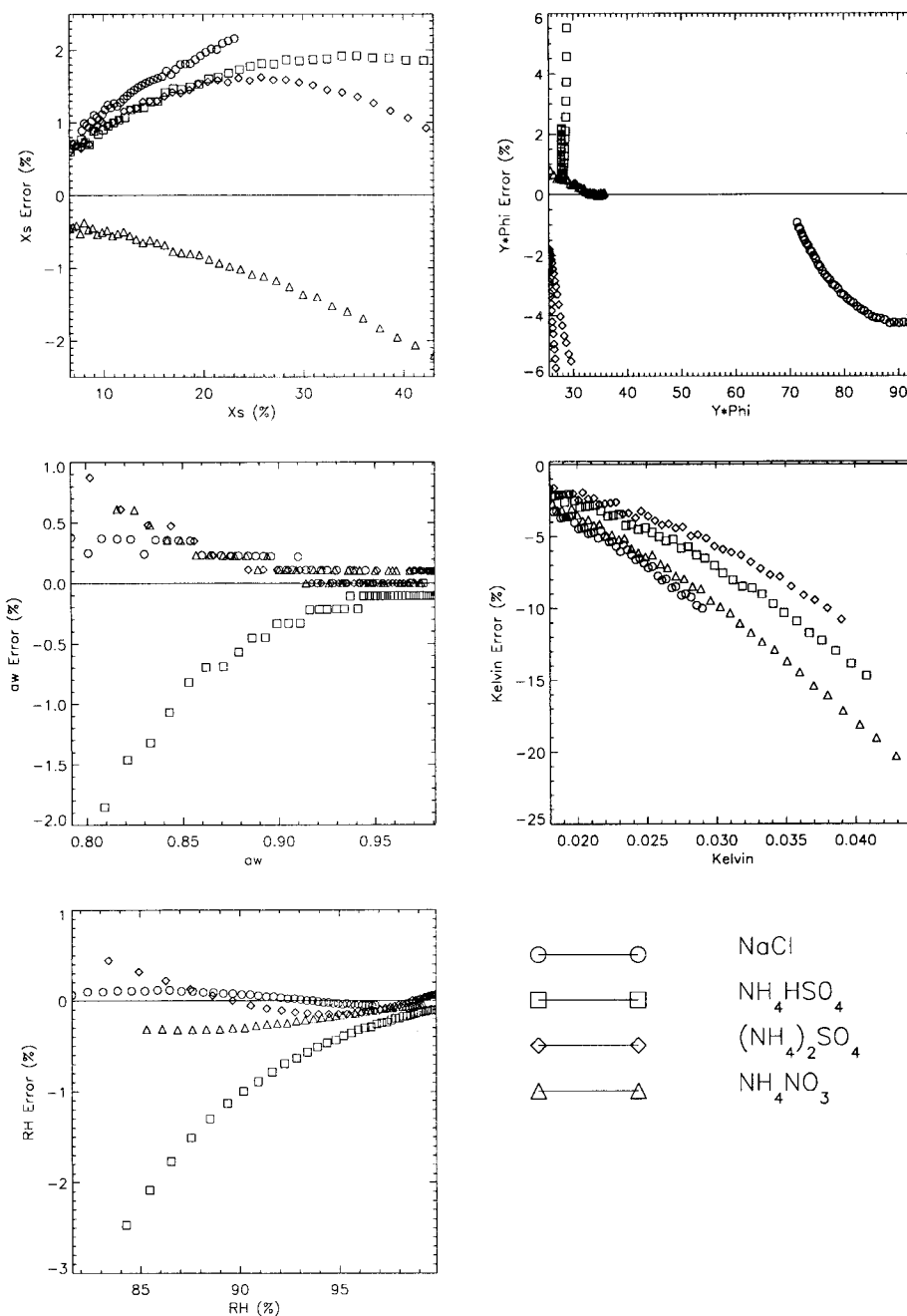


FIG. 3. Errors (%) in x_s , Φ , a_w , natural log of Kelvin term, and RH due to assumptions of volume additivity, $\bar{\sigma}_{\text{drop}} = \sigma_w$, and $\Phi = \Phi_j$, for different solute chemical compositions studied. Circles designate NaCl, squares designate NH₄HSO₄, diamonds designate (NH₄)₂SO₄, and triangles designate NH₄NO₃. A dry particle size of 40 nm was assumed for all calculations. Solid horizontal lines designate 0% error.

the two different methods for calculating RH, therefore, the percent error in RH is presented in Fig. 3. Results in Fig. 2a demonstrate agreement between the two different methods for determining RH within 0.5% for NaCl and (NH₄)₂SO₄ over the range of RHs experienced during HTDMA studies. The agreement for NH₄HSO₄ and NH₄NO₃ is not as good as for the other solutes, but

still between 0% and 2.5%. Uncertainties in the values of a_w and RH determined from the reference model are estimated between $\pm 1\%$ and $\pm 2.5\%$, based on errors in Pitzer's model of Φ , and errors in the polynomial fits to solution density data.

The RH values predicted by the reference Köhler model for internally mixed solutes were compared with

results from the ZSR relation (Stokes and Robinson 1966). In the ZSR relation, the assumption is made that the total water uptake by an internally mixed composition particle is equal to the sum of the water uptake by the individual solutes. The total mass fraction of solute in the ternary solution (x_s) was determined for the assumed mass fractions of solutes a and b in the dry particle and for a given drop diameter by iteratively solving Eq. (18), and using Eq. (15) to compute ρ_{drop} . First, the mass fractions of solutes a and b in the dry particle were fixed. To calculate ρ_s , Eq. (13) was used. The total mass of solute could then be determined for the assumed dry particle size and the calculated value of ρ_s , assuming the particle was spherical in shape. Next, for an assumed value of D_{drop} , an initial guess for the water content was proposed, from which x_s was calculated. The value of ρ_{drop} in Eq. (15) corresponding to x_s could then be determined. The Newton–Raphson technique was used to iteratively solve for the value of x_s in Eq. (18) so that the difference between the two terms on the left side was less than 10^{-6} . The value of x_s determined from the iteration was then used to calculate the solution molality, m , and the solution density. Using the polynomials of molality as a function of water activity from Tang and Munkelwitz (1994) in the ZSR relation, the water activity solving the ZSR relation was determined using the following form

$$\frac{f_a m}{m_{a,0}} + \frac{f_b m}{m_{b,0}} = 1, \quad (19)$$

where $m_{a,0}$ and $m_{b,0}$ are the molalities of the binary solutions of solutes a and b calculated using Tang's polynomials as a function of a_w for the given water activity. Equation (19) was solved iteratively using a procedure similar to that outlined above, and the value of a_w corresponding to x_s determined. The RH corresponding to the value of a_w was then calculated by applying the Kelvin correction as shown in Eq. (1). We note that the form of the ZSR relation given by Eq. (19) does not account for interactions between the two solutes in solution. According to Tang (1997), the assumption that the solutes in ternary solutions do not interact can lead to errors in predicted values of a_w using the ZSR relation between 1% and 6%. Tang (1997) presents results for an extended ZSR relation that better fits experimental data of a_w as a function of m for a variety of mixed solutes in ternary solutions where the two solutes have one common ion.

Values of RH determined from the ZSR relation using Tang's density and water activity polynomials are compared with those from the reference model for ternary solutions in Fig. 2b. In the figure, the ZSR results are shown as dotted lines and the reference model results are shown as solid lines. The percent difference between the RH values calculated using the two different techniques is shown in the right column. The agreement between the ZSR-predicted and reference model-pre-

dicted RHs is not as good as for the single solutes examined. For the last three mixtures examined, the percent error in RH is less than 3.3% for the RH range 80%–92%. Better agreement is found at a higher RH, corresponding to more dilute solutions where the assumption that the osmotic coefficient of the ternary solution can be determined by the molality weighting approach is more valid. For the one case where the extended version of the ZSR relation was used (NaCl–Na₂SO₄–H₂O), the agreement is worse than that found for the other ternary solutions, but is within 2% for RH's greater than 89%. This demonstrates that interactions between solutes in solution can be important for ternary solutions. Parameters for the extended ZSR relation are not available for any of the other ternary solutions examined.

5. Development of the modified Köhler model

In this section we describe the simplifying assumptions made to the reference Köhler model and our methodology for testing their validity. The assumptions include volume additivity of solute and solvent within the drop; substitution of the surface tension of pure water for the solution surface tension; and the use of a simplified, parameterized form of the osmotic coefficient in the Raoult term. The sensitivity of predicted values of RH to the various assumptions is examined for particles composed of single solutes. The validity of the assumptions is checked over the range of RHs of HTDMA studies (80%–92%) to ensure that the final modified Köhler model can accurately describe the hygroscopic growth of particles over this range.

a. Assumption of volume additivity

Assuming the volumes of solute and solvent may be added to determine the solution total volume is equivalent to assuming the partial molar volume of water in solution is equal to the molar volume of pure water. If volume additivity is assumed, the mass fraction may be determined as follows:

$$x_s = \frac{\rho_s D_{p,\text{sol}}^3}{\rho_w (D_{\text{drop}}^3 - D_{p,\text{sol}}^3) + \rho_s D_{p,\text{sol}}^3}, \quad (20)$$

where ρ_w is the density of pure water. The partial molar volume of water for a variety of solution compositions is shown in Fig. 1. The difference between the partial molar volume of water and the molar volume of pure water increases with increasing mass fraction. The largest difference is found for (NH₄)₂SO₄ and amounts to –4% for $x_s = 40\%$.

We tested the sensitivity of values of x_s , Φ , a_w , the natural log of the Kelvin term, and equilibrium RH predicted by Eq. (9) using the Pitzer model for Φ to the assumption of volume additivity. Calculations show that differences in x_s when volume additivity is assumed lead

to maximum errors in Φ of about 1%, with similar errors propagating to a_w . The Kelvin term depends on x_s through $\bar{\sigma}_{\text{drop}}$ and exhibits relatively larger error than a_w . However, for RHs below 95% the Kelvin term has a relatively smaller effect on the predicted equilibrium RH than the Raoult term, so the influence of the error in the Kelvin term on RH is very small. The errors in equilibrium RHs due to the assumption of volume additivity are between 0.6% and -0.9% , which is smaller than uncertainties in the reference model RH values. The differences between the reference RHs and RHs predicted by the modified Köhler model assuming volume additivity were found to decrease with increasing RH, consistent with the fact that as the solution becomes more dilute, the assumption that the volumes may be added becomes more valid. Based on the results of this analysis, the assumption of volume additivity is made in this work, therefore, the molar volume of pure water is used in place of \bar{v}_l .

b. Assumption of $\bar{\sigma}_{\text{drop}} = \sigma_w$

As shown in Fig. 1, for the solute mass fraction range encountered in HTDMA studies, the difference between $\bar{\sigma}_{\text{drop}}$ and σ_w can be as high as 28% for NH_4NO_3 . This difference is similar to the maximum difference noted by Schulmann et al. (1996) between the surface tensions of various organic acid aqueous solutions and pure water. Assuming $\bar{\sigma}_{\text{drop}} = \sigma_w$ only affects the Kelvin term and equilibrium RH. Although the errors in the Kelvin term are similar to the differences between $\bar{\sigma}_{\text{drop}}$ and σ_w in Fig. 1, the associated error in RH is small because the Kelvin term is relatively smaller than the Raoult term. As the solution becomes more dilute, the assumption that $\bar{\sigma}_{\text{drop}} = \sigma_w$ becomes more valid. The maximum error in RH incurred by assuming $\bar{\sigma}_{\text{drop}} = \sigma_w$ (-1.5%) is less than the maximum uncertainty in the reference model RH values, therefore we assume that $\bar{\sigma}_{\text{drop}} = \sigma_w$, equivalent to setting $b = 0$ in the reference Köhler model.

c. Parameterization of Φ

The full model for Φ [Eq. (7)] is too complex to be easily applied to determining S_{crit} from HTDMA study results. Pitzer and Mayorga (1973) suggest that for most solutes and solution ionic strengths below 6 molal, the term involving m^2 is very small and may be neglected; therefore, we do so. Furthermore, our investigations show that for solution ionic strengths encountered in our studies, the β_1 term is very small compared to the β_0 term; therefore, we choose to set $\beta_1 = 0$. With the above simplifications, the original expression for Φ , Eq. (7), becomes

$$\Phi = 1 - |z_1 z_2| \left[A_\phi \frac{\sqrt{I}}{1 + b_{\text{pit}} \sqrt{I}} \right] + m \frac{2\nu_1 \nu_2 \beta_0}{\nu} \quad (21)$$

Values of Φ predicted by the truncated expression, Eq.

(21), were compared with those from Eq. (7). Calculations were performed for RH values between 80% and slightly over 100% for all of the compositions investigated in this work as well as for H_2SO_4 . For H_2SO_4 , the two neglected terms in Pitzer's model are important, and poor agreement was found between the full and simplified versions of Φ at RHs below 99%. Therefore, the proposed simplified version of Φ cannot be applied to particles composed of H_2SO_4 . For NaCl , NH_4HSO_4 , $(\text{NH}_4)_2\text{SO}_4$, NH_4NO_3 , and the internally mixed solutes examined here, Eq. (21) reproduced the values of Φ from the full Pitzer model within 10% for all compounds except NH_4HSO_4 and internally mixed $\text{NaCl-Na}_2\text{SO}_4$. The worst agreement was for NH_4HSO_4 , where Φ was overpredicted by as much as 19% at an RH of 80%. For the binary solutions examined, the simplified model for Φ tended to overpredict Φ for RHs between 80% and 92%. Overpredictions of Φ will result in underpredictions of S_{crit} since the larger values of Φ will effectively increase the solute effect, resulting in a lower predicted equilibrium RH for a given solution composition. The maximum errors in Φ corresponded to smaller maximum errors, within -2.5% , in predicted values of a_w and RH. The maximum errors in a_w and RH were found for NH_4HSO_4 and $(\text{NH}_4)_2\text{SO}_4$, and were due to the relatively poorer approximation made in using Eq. (21) to determine Φ . At 92% RH, the maximum errors in a_w and RH were $\pm 0.5\%$.

Assuming volume additivity in Eq. (4), and an using relations for the masses of solute (m_s) and water (m_w) in the droplet, the molality, m , may be written

$$m = \frac{1000\rho_s D_{p,\text{sol}}^3}{M_s \rho_w (D_{\text{drop}}^3 - D_{p,\text{sol}}^3)}, \quad (22)$$

where ρ_w is the density of pure water. We can define a coefficient c as

$$c = \frac{1000D_{p,\text{sol}}^3}{\rho_w (D_{\text{drop}}^3 - D_{p,\text{sol}}^3)}, \quad (23)$$

which can be calculated for each HTDMA (D_{drop} , RH) data pair for a known $D_{p,\text{sol}}$. The solution molality may be rewritten in terms of c ,

$$m = \frac{\rho_s c}{M_s}, \quad (24)$$

and the ionic strength of a solution with a solute dissociating into two ions may be written

$$I = \frac{1}{2} \sum m_i z_i^2 = \frac{1}{2} [z_1^2 \nu_1 + z_2^2 \nu_2] \frac{\rho_s c}{M_s}, \quad (25)$$

since the molality of each of the ionic species in solution (m_i) is just the solution molality (m) multiplied by the number of ions from the dissociation of one molecule of the solute (ν_i). Substituting the above expressions for m and I into Eq. (21) we find

TABLE 4. Values of $Y = \nu\rho_s/M_s$, β_0 , Y_a , Y_b , Y_c , Y_f , and $\beta_{0,f}$ for solute chemical compositions examined in this work. The units of all Y parameters are 10^{-3} m^{-3} and β_0 is dimensionless. Values of Y_f and $\beta_{0,f}$ were determined by fitting the product $Y_f\Phi_f$ to calculated values of the product $Y\Phi$.

Solute	Y	β_0	Y_a	Y_b	Y_c	Y_f	$\beta_{0,f}$
NaCl	74.09	0.1082	74.1	74.1	18.52	77.4	0.018
$(\text{NH}_4)_2\text{SO}_4$	40.16	0.04763	321.3	80.3	8.93	29.1	0.008
NH_4HSO_4	30.93	0.04494	30.93	30.93	7.73	33.3	0.006
H_2SO_4	56.35	-0.0933	450.8	112.7	12.5	2.0	21.8
NH_4NO_3	43.10	-0.0154	43.1	43.1	10.78	44.1	-0.004
$\text{NaCl}-(\text{NH}_4)_2\text{SO}_4$	49.2	0.078	197.7	77.2	13.7	43.1	0.013
$(\text{NH}_4)_2\text{SO}_4-\text{NH}_4\text{NO}_3$	41.3	0.016	182.2	61.7	9.9	36.3	-0.002
$\text{NaCl}-\text{NH}_4\text{NO}_3$	54.5	0.046	58.6	58.6	14.6	57.6	0.006
$\text{NaCl}-\text{Na}_2\text{SO}_4$	62.5	0.064	263.5	93.7	15.6	45.9	0.03

$$\Phi = 1 - |z_1 z_2| \left[A_\phi \frac{\sqrt{\frac{1}{2}[z_1^2 \nu_1 + z_2^2 \nu_2] \frac{\rho_s c}{M_s}}}{1 + b_{\text{pit}} \sqrt{\frac{1}{2}[z_1^2 \nu_1 + z_2^2 \nu_2] \frac{\rho_s c}{M_s}}} \right] + \frac{2\nu_1 \nu_2 \beta_0 \rho_s c}{\nu M_s} \quad (26)$$

Equations (25) and (26) are explicitly written for a solute that dissociates into two ions in solution.

In an effort to further simplify the form for Φ given by Eq. (21), we define different parameters, Y_i , and substitute them into Eq. (26). In the numerator of the Debye-Hückel term, a parameter Y_a can be defined for a solute molecule that dissociates into two ions,

$$Y_a = |z_1 z_2|^2 [\nu_1 z_1^2 + \nu_2 z_2^2] \frac{\rho_s}{M_s}, \quad (27)$$

while in the denominator a parameter Y_b can be defined as

$$Y_b = [\nu_1 z_1^2 + \nu_2 z_2^2] \frac{\rho_s}{M_s}. \quad (28)$$

In the β_0 term, a parameter Y_c can be defined as

$$Y_c = \frac{\nu_1 \nu_2 \rho_s}{\nu M_s}. \quad (29)$$

The theoretically correct values of Y_a , Y_b , and Y_c are shown in Table 4. Substituting the above definitions for each of the Y_i into Eq. (26), we find Eq. (30), equivalent to Eq. (21):

$$\Phi = 1 - \frac{A_\phi \sqrt{Y_a c}}{\sqrt{2} + b_{\text{pit}} \sqrt{Y_b c}} + 2Y_c \beta_0. \quad (30)$$

The above definitions of Y_a , Y_b , and Y_c have the common factor ρ_s/M_s and prefactors involving ν_i and z_i that depend upon the chemical composition of the solute. Furthermore, the common factor also appears in the coefficient of Φ in the reference Köhler model [Eq. (9)] through x_s and M_s . We define the following unknown variable

$$Y = \frac{\nu \rho_s}{M_s}. \quad (31)$$

Values of Y are listed in Table 4. The various Y_i differ from Y by a constant that depends on the ratio of cations to anions for a given solute. Although a single definition of the combination of ν_i , z_i , and ρ_s/M_s cannot be substituted into Eq. (30) for Φ for the different Y_i , we substitute a single unknown Y_f for each of the Y_i and assume that the retained functional dependence on ρ_s/M_s of the resulting parameterization is sufficient to accurately model the variation of Φ with RH for HTDMA conditions and to predict S_{crit} . This assumption is tested below in our numerical simulations of the derivation of S_{crit} . In the modified Köhler equation, the product $\Phi_f Y_f c = m\Phi_f$ will be substituted for the product of molality and Φ . With all of the aforementioned assumptions, the parameterized form for Φ becomes

$$\Phi_f = 1 - \frac{A_\phi c^{1/2} Y_f^{1/2}}{\sqrt{2} + b_{\text{pit}} c^{1/2} Y_f^{1/2}} + 2c\beta_{0,f} Y_f, \quad (32)$$

where Φ_f denotes the proposed simplified form for Φ , and Y_f and $\beta_{0,f}$ are the only unknowns and depend only on the dry particle chemical composition. Note that in the above equation for Φ_f , the parameter $\beta_{0,f}$ no longer has the same value as Pitzer's β_0 coefficient if the single definition of Y_f is used. Although b_{pit} , another adjustable parameter in Pitzer's model, would also be different in Φ_f , we assume the same value used by Pitzer.

To test the validity of assuming $Y_f = Y_a = Y_b = Y_c$ in Eq. (32), we fit the product $Y_f \Phi_f$ to data of $Y\Phi$ as a function of x_s and determined best-fit values of Y_f and $\beta_{0,f}$. The product $Y_f \Phi_f$ was fit since it is this product that appears in the relation for a_w . All terms are retained in the osmotic coefficient expression used to calculate the product $Y\Phi$. The $D_{p,\text{sol}}$, D_{drop} pairs were chosen for a given solute chemical composition and Φ calculated as a function of molality using the full Pitzer model. The fits were performed for molality ranges expected during HTDMA conditions, between approximately 1 and 6 molal. Best-fit values of Y_f and $\beta_{0,f}$ are shown in Table 4 for each solute. Except for H_2SO_4 , Y_f tends to be close to Y , suggesting that some information about

the chemical composition of the particle nuclei can be inferred from the fit of $Y_f\Phi_f$ to $Y\Phi$ data.

Differences were examined between values of a_w and RH predicted using the full model for $Y\Phi$ and those calculated using the best-fit parameters in $Y_f\Phi_f$. The best-fit values of Y_f and $\beta_{0,f}$ shown in Table 4 were used in Eq. (32) to calculate Φ_f , and the product of c , Y_f , and Φ_f was then used in place of the product of m and Φ to calculate a_w [Eq. (2)]. This value of a_w was substituted into Eq. (1) to examine how errors in a_w propagated to errors in RH. The maximum errors in a_w and RH were between +1% and -2.5%, similar to the uncertainties in the reference model values for these parameters. Based on these results, we accept the proposed parameterization of Φ_f , Eq. (32), for use in the modified Köhler model.

d. Combined assumptions of $\bar{v}_i = v_w$, $\bar{\sigma}_{drop} = \sigma_w$, and $\Phi = \Phi_f$

In Fig. 3 we explore errors in the various parameters when all of the aforementioned assumptions are made simultaneously. Each chemical composition is represented by a different symbol in the figure. Results are reported as percent error relative to the values from the reference model for the same dry and wet particle sizes. The errors in a_w and RH are between 0% and 1% and $\pm 0.5\%$, respectively, for all compounds except NH_4HSO_4 . The errors for NH_4HSO_4 are relatively larger due to the relatively poorer approximation made for this compound, as discussed above. Based on the results shown in Fig. 3, except for NH_4HSO_4 , the modified Köhler model is shown to correctly predict RH and a_w within reference model uncertainties ($\pm 3\%$) and experimental uncertainties in RH ($\pm 1\%$) during HTDMA studies.

e. Modified form of Köhler equation

Substituting the above relation for Φ_f [Eq. (32)] into Eq. (9) and incorporating the simplifications discussed in the previous section, the Köhler equation for a droplet containing a single, completely dissociated solute may be written

$$\text{RH} = 100 \exp\left[\frac{4\sigma_w M_w}{\rho_w RT D_{\text{drop}}}\right] \times \exp\left[\frac{-M_w c}{1000} \left(Y_f - \frac{A_\phi c^{1/2} Y_f^{3/2}}{\sqrt{2} + b_{\text{pit}} c^{1/2} Y_f^{1/2}} + 2c\beta_{0,f} Y_f^2\right)\right], \quad (33)$$

where c is defined as

$$c \equiv \frac{1000 D_{p,\text{sol}}^3}{\rho_w (D_{\text{drop}}^3 - D_{p,\text{sol}}^3)}. \quad (34)$$

In the above equations, M_w , R , and b_{pit} are constants;

$D_{p,\text{sol}}$, D_{drop} , RH, and T are measured during HTDMA studies; σ_w , ρ_w , and A_ϕ are a function of T only; and c is known if $D_{p,\text{sol}}$, ρ_w , and D_{drop} are known. This leaves Y_f and $\beta_{0,f}$ as the two chemical composition-dependent unknowns that remain to be determined. By fitting Eq. (33) to $(D_{\text{drop}}, \text{RH})$ data pairs determined from HTDMA studies performed on the same monodisperse dry particle size at different RHs, the two unknowns, Y_f and $\beta_{0,f}$ may be determined. Once known, the values of Y_f and $\beta_{0,f}$ may be used in Eq. (33) to find the maximum equilibrium RH, which is S_{crit} .

Another, simpler Köhler model was proposed by Weingartner et al. (1997) to fit HTDMA study results in order to derive S_{crit} . It is of interest to compare the results from their model with those from the model proposed in this work. Their model took the form

$$\text{RH} = 100 \exp\left[\frac{\alpha}{D_{\text{drop}}}\right] \exp\left[\frac{-\beta N_i}{D_{\text{drop}}^3 - D_{p,\text{sol}}^3}\right], \quad (35)$$

where α was taken equal to 2.155 nm, β was set equal to $5.712 \times 10^{-2} \text{ nm}^3$, and the droplet and particle sizes were in nanometers (Weingartner et al. 1997). The number of dissociated molecules in the water layer of the droplet, N_i , was the one unknown in the model. By comparison of Eqs. (35) and (33), N_i is defined as

$$N_i \equiv Y N_{\text{av}} \frac{\pi}{6} D_{p,\text{sol}}^3, \quad (36)$$

where N_{av} is Avogadro's number and Y is defined by Eq. (31). Implicit in the form of Eq. (36) is the assumption that Φ is constant and does not vary with RH, whereas the variation of Φ with RH is built into the modified Köhler model proposed in this work [Eq. (33)]. Below, we compare theoretical values of S_{crit} predicted by the reference Köhler model to values of S_{crit} derived by fitting Eqs. (33) and (35) to $(D_{\text{drop}}, \text{RH})$ data pairs representing hypothetical HTDMA study results.

6. Estimating S_{crit} using simulated HTDMA data

For the numerical sensitivity studies, a dry particle size and composition were chosen. The reference Köhler model was used to calculate the theoretical equilibrium RH for assumed droplet sizes. The $(D_{\text{drop}}, \text{RH})$ data pairs and the assumed dry particle size were used in a nonlinear, least squares fit routine to derive values of Y_f and $\beta_{0,f}$ in Eq. (33) and N_i in Eq. (35). Two input data pairs were insufficient to capture the curvature of the Köhler curve. Ten pairs were used for each of the sensitivity studies described below. Trial and error sensitivity studies on the minimum number of input data pairs required to maintain acceptable error in derived values of S_{crit} from Eq. (33) showed that 3 input data pairs equally spaced between 80% and 92% RH produced the same error in S_{crit} as 10 data pairs over the same RH range.

Four different cases were investigated. First, we determined Y_f and $\beta_{0,f}$ from a fit of Eq. (33) with perfect

input values for $D_{p,\text{sol}}$, D_{drop} , and RH. Second, we verified that the results from the fit routine were not sensitive to the initial guess for Y_f and $\beta_{0,f}$. Third, we determined the sensitivities of the derived values for Y_f and $\beta_{0,f}$ to assumed $\pm 0.5\%$ random errors in RH, D_{drop} , and $D_{p,\text{sol}}$. Fourth, we examined the sensitivity of derived values of the unknowns to $\pm 1\%$ random error in RH, dry particle size, and droplet size. The random errors in the three input parameters were applied simultaneously, and the values chosen were guided by expected experimental error. As discussed in Part II, the observed, average experimental uncertainty in RH during laboratory HTDMA studies was $0.7\% \pm 0.2\%$, therefore, the 0.5% – 1% range of applied random RH error is relevant for investigating the influence of RH uncertainties on fit routine results. The model of Weingartner et al. (1997) and that proposed in this work were run simultaneously only for the fourth case, and dry particle sizes of 40 and 100 nm were examined. For studies on internally mixed particles, only the cases described above with perfect input and with assumed $\pm 1\%$ random uncertainties applied to all input data were investigated. These uncertainties were chosen to reflect those expected in experimental data. Rader and McMurry (1986) have studied the sizing errors in the TDMA. They determined that the error in the measured midpoint diameter in the second DMA was $0.11\% \pm 0.06\%$ for particle diameters less than 200 nm. For flow uncertainties in the HTDMA measurement system, the estimated experimental uncertainty in particle sizing is between 0.2% and 1%.

A single case study of the effect that a single set of applied random errors has on values of Y_f , $\beta_{0,f}$, and S_{crit} from the fit procedure would be less representative of the average influence of experimental uncertainties than averaging the results from several cases of assumed random errors. Therefore, 100 cases were run on the same input $D_{p,\text{sol}}$, D_{drop} , and RH data for each assumed range of random errors in order to obtain a statistically significant estimate of the influence of uncertainties on the derived values of Y_f and $\beta_{0,f}$.

Results from our numerical simulations are shown in Table 5 for dry diameters of 40 and 100 nm. The values of Y_f and $\beta_{0,f}$ in Table 5 for the cases of perfect input, are close to, but not exactly the same as values in Table 4. The reason for this is that the values in Table 4 were determined by fitting the product of $Y_f\Phi_f$ to values of $Y\Phi$ as described above, whereas the values in Table 5 were determined by fitting the modified Köhler model to (D_{drop} , RH) data pairs calculated using the reference model. The values of Y_f and $\beta_{0,f}$ shown in the table for cases where errors were applied are obtained by averaging the results from the 100 different cases of applied error. Ratios of the standard deviation computed from the 100 different cases to the average values of Y_f , $\beta_{0,f}$, and S_{crit} were less than 0.2, 1.3, and 0.16, respectively. The small standard deviations for Y_f and S_{crit} indicate that the fit routine is quite stable.

The relatively larger value for $\beta_{0,f}$ is due to the lower sensitivity of the goodness of fit to the value of this parameter compared to Y_f . Tests of the sensitivity of the fit routine to assumed initial conditions showed it to be insensitive, therefore, we report results from these cases for NaCl only. For the cases with $D_{p,\text{sol}} = 100$ nm, there were no significant differences between results where $\pm 0.5\%$ and $\pm 1\%$ random errors were applied; therefore, only results for cases with $\pm 1\%$ errors are shown.

Values of the critical droplet diameter (D_{crit}) are shown in Tables 5 and 6 for the single and mixed solutes examined. The results demonstrate that the fit routine derived values of Y_f and $\beta_{0,f}$ return values of D_{crit} that agree with theoretical values within -10% and 12% when used in the modified Köhler model. Also shown in the tables is the χ^2 convergence value of the fit in units of RH. In general, the χ^2 values are smaller than 0.5%; however, for NH_4NO_3 the values for the case with perfect input data are larger. This is most likely due to the poorer approximations made by assuming volume additivity (x_i , Fig. 3) and $\bar{\sigma}_{\text{drop}} = \sigma_w$ (Fig. 1) for NH_4NO_3 compared to other solutes.

The percent errors in derived values of S_{crit} are listed in Table 5 for the five different single solute compositions examined and in Table 6 for the mixed solutes examined. For comparison, values of S_{crit} from the reference Köhler model are listed in Table 3 for the various dry particle sizes and chemical compositions examined. Results of the fit routine using the modified Köhler model of this work and applied error have been plotted as solid dots in Fig. 4, with the solid line designating the 1:1 line. The results from the model of Weingartner et al. (1997) with applied error are shown as squares in the figure and are discussed below. The plus symbols designate results where no errors were applied to the input data. Results from the model of this work and an assumed 40-nm-diameter particle have been labeled in Fig. 4 with the corresponding chemical composition for particles composed of single solutes. Results from the model with internally mixed solutes are not labeled in Fig. 4. As can be seen from the figure, the agreement between theoretical and predicted values of S_{crit} is very good. Also, the results for the cases where no errors were applied are similar to those with error. Therefore, the assumed uncertainties in the input data do not adversely affect the ability of the fit routine and modified Köhler model to predict accurate values of S_{crit} . The errors in predicted values of S_{crit} are between -20% and $+15\%$, similar to the uncertainties in experimental estimates of S_{crit} determined from CCN studies on known particles (-0.6% , $1\sigma = 11\%$, $n = 16$; Brechtel and Kreidenweis 2000). For comparison, the supersaturations in a typical stratocumulus cloud can vary between 0.1% and 1% (Rogers and Yau 1989). Although cloud supersaturations cannot be measured directly, Yum et al. (1998) have estimated supersaturations and standard deviations of supersaturations for stratocumulus clouds

TABLE 5. Sensitivity of fit routine results as a function of particle composition, initial guess and assumed $D_{p,sol}$, RH and D_{drop} errors for 40- and 100-nm dry particle diameters and indicated compositions. Ratios of the standard deviation computed from the 100 different cases of applied error to the average values of Y_f , $\beta_{0,f}$, and S_{crit} were always less than 0.2, 1.3, and 0.16, respectively. Input RHs were calculated using the reference model. The simplified Köhler model was run with initial conditions equal to five times the perfect initial conditions for the cases including assumed uncertainties.

Case	$D_{p,sol}$ (nm)	Y_f	$\beta_{0,f}$	S_{crit} (%)	Error (%)	D_{crit} (nm)	Error (%)	χ^2
Sodium Chloride								
Perfect input	40	81.653	0.01488	0.43	-10	315	-1	5.22×10^{-1}
5 × ICs	40	81.653	0.01488	0.43	-10	315	-1	5.22×10^{-1}
0.5% error	40	80.944	0.01532	0.43	-10	316	-1	3.67×10^{-2}
1% error	40	78.504	0.01754	0.43	-9	313	-2	3.90×10^{-1}
Perfect input	100	80.098	0.01598	0.11	-9	1265	-1	7.14×10^{-1}
1% error	100	78.349	0.01838	0.11	-8	1251	-2	3.63×10^{-1}
Ammonium Sulfate								
Perfect input	40	28.723	0.01023	0.65	-8	208	0	2.84×10^{-1}
0.5% error	40	28.549	0.01059	0.65	-7	208	0	4.02×10^{-2}
1% error	40	28.367	0.01086	0.65	-7	206	-1	4.88×10^{-1}
Perfect input	100	28.295	0.01093	0.16	-5	839	-4	2.66×10^{-1}
1% error	100	26.889	0.01374	0.17	-2	816	-7	3.62×10^{-1}
Ammonium Bisulfate								
Perfect input	40	35.801	0.00064	0.58	-20	232	10	7.48×10^{-3}
0.5% error	40	35.653	0.00068	0.58	-20	231	10	3.70×10^{-2}
1% error	40	34.939	0.00099	0.59	-19	229	9	3.75×10^{-1}
Perfect input	100	34.784	0.00158	0.15	-20	929	12	1.09×10^{-3}
1% error	100	32.987	0.00307	0.15	-19	918	10	3.84×10^{-1}
Sulfuric Acid								
Perfect input	40	37.340	0.05529	0.56	-7	243	1	8.14×10^{-1}
0.5% error	40	36.843	0.05864	0.56	-6	241	0	9.18×10^{-2}
1% error	40	33.323	0.08634	0.59	-1	232	-2	3.82×10^{-1}
Perfect input	100	35.986	0.06038	0.14	0	951	-8	1.46
1% error	100	34.050	0.08118	0.15	1	934	-10	3.80×10^{-1}
Ammonium Nitrate								
Perfect input	40	44.386	-0.00418	0.52	-2	258	1	4.25
0.5% error	40	44.201	-0.00419	0.52	-2	258	1	1.91×10^{-2}
1% error	40	42.899	-0.00415	0.53	0	252	0	3.31×10^{-1}
Perfect input	100	44.073	-0.00388	0.13	-2	1047	1	1.44
1% error	100	42.812	-0.00377	0.13	-2	1045	1	3.36×10^{-1}

from measurements of CCN spectra, cloud droplet spectra, and other parameters. The results of Yum et al. (1998) showed that predicted standard deviations in supersaturations were between 40% and 100% of the predicted supersaturations. The reported standard deviations may be representative of the variability in supersaturations in clouds, and we note that the modified Köhler model of this work can predict values of S_{crit} with lower uncertainty.

In Fig. 4, the S_{crit} values from the modified Köhler model of this work for particles composed of single solutes are typically underpredicted by the fit routine. This is caused by the systematic underprediction of the Kelvin term due to the assumption that the surface tension of the solution is equal to that for pure water and by the overprediction of Φ by the assumed simplified form, Φ_f . The average agreement between predicted and theoretical values of S_{crit} for all compounds listed in Tables 5 and 6 is -7.5% ($1\sigma = 10\%$, $n = 9$). A surprising result in Table 5 is the relatively good agreement between predicted and theoretical values of S_{crit} for

H_2SO_4 , especially given the poor agreement between values of Φ from the full Pitzer model and values calculated using the simplified model of Φ . The values of Y_f and $\beta_{0,f}$ in Table 5 are significantly different from the values of Y and β_0 and the values of Y_f and $\beta_{0,f}$ in Table 4. Even though the parameterization for Φ does not accurately reproduce the actual behavior of Φ for H_2SO_4 , for this compound fit parameters could be derived that allowed the modified Köhler model to accurately reproduce the droplet growth with increasing RH as well as values of S_{crit} . The results in Fig. 4 demonstrate that for a single dry particle size, the various compositions examined correspond to about a factor of 2 change in S_{crit} . Therefore, particle chemical composition plays an important role in determining critical supersaturation.

The largest errors in predicted values of S_{crit} are found for NH_4HSO_4 and internally mixed $NaCl-Na_2SO_4$. This is not surprising for at least three reasons. First, it is possible that the modified Köhler model is less capable of capturing the hygroscopic behavior of certain particle

TABLE 6. Sensitivity of fit routine results as a function of particle composition, and assumed $D_{p,sol}$, RH, and D_{drop} errors for 40- and 100-nm dry particle diameters and indicated equimolar mixtures of solutes. Ratios of the standard deviation computed from the 100 different cases of applied error to the average values of Y_f , $\beta_{0,f}$, and S_{crit} were always less than 0.2, 1.3, and 0.16, respectively. The input RHs used in the fit routine were calculated using the reference model. The simplified Köhler model was run with initial conditions equal to the perfect initial conditions for the cases including assumed uncertainties.

Case	$D_{p,sol}$ (nm)	Y_f	$\beta_{0,f}$	S_{crit} (%)	Error (%)	D_{crit} (nm)	Error (%)	χ^2
Sodium Chloride–Ammonium Sulfate								
Perfect input	40	43.140	0.01317	0.74	4	183	10	0.589
With 1% error	40	40.835	0.01727	0.76	7	177	6	0.376
Perfect input	100	42.096	0.01456	0.19	5	728	0	0.691
With 1% error	100	40.336	0.01719	0.19	6	718	-1	0.337
Ammonium Sulfate–Ammonium Nitrate								
Perfect input	40	36.247	-0.00233	0.81	3	166	12	0.148
With 1% error	40	34.850	-0.00169	0.83	6	162	10	0.301
Perfect input	100	35.611	-0.00183	0.20	4	670	1	0.119
With 1% error	100	33.536	-0.00043	0.21	6	654	-1	0.279
Sodium Chloride–Ammonium Nitrate								
Perfect input	40	57.578	0.00625	0.64	0	210	12	0.107
With 1% error	40	55.991	0.00734	0.64	0	210	12	0.336
Perfect input	100	56.508	0.00717	0.16	-1	848	5	0.171
With 1% error	100	54.910	0.00823	0.16	-1	845	5	0.302
Sodium Chloride–Sodium Sulfate								
Perfect input	40	45.869	0.03092	0.71	13	190	0	1.52
With 1% error	40	45.040	0.03302	0.72	15	188	-1	0.379
Perfect input	100	46.140	0.02974	0.18	13	766	-8	1.01
With 1% error	100	44.288	0.03403	0.18	15	758	-9	0.432

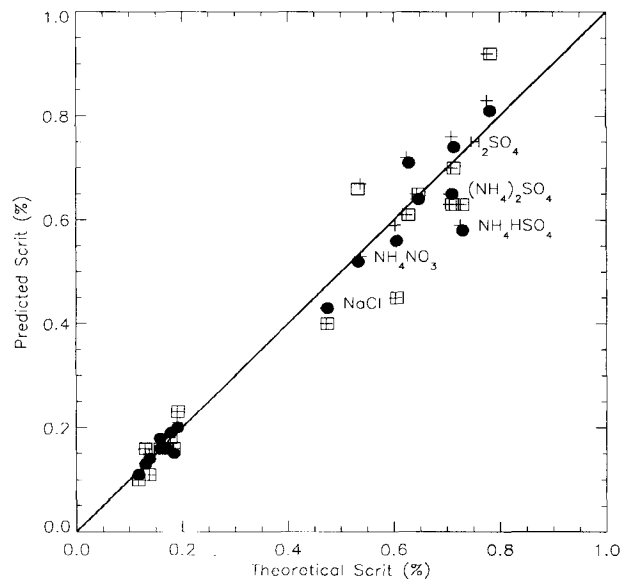


FIG. 4. Values of S_{crit} from proposed Köhler model and fit routine vs theoretical values of S_{crit} for 40- and 10-nm-diameter particles and all chemical compositions examined in this work. Solid dots represent results from Köhler model of this work with applied error and squares represent results from model of Weingartner et al. (1997) with applied error. Solid line is 1:1 line. Plus symbols represent results with no applied errors to the input data. Results for 40-nm internally mixed solutes are not labeled.

chemical compositions compared to others. Second, the full Pitzer model of Φ is less accurate for NH_4HSO_4 (Kim et al. 1993). Third, (other than H_2SO_4) NH_4HSO_4 and internally mixed NaCl – Na_2SO_4 compositions exhibited the poorest agreement between values of Φ from the full Pitzer model and values calculated using the simplified model of Φ . The underprediction of Φ by the simpler model for internally mixed NaCl – Na_2SO_4 results in an overprediction of S_{crit} .

Comparison of results from different Köhler models

The same numerical sensitivity studies conducted with the modified Köhler model proposed here were performed on the model proposed by Weingartner et al. (1997). Results from their model are shown in Fig. 4 as squares and demonstrate reasonable agreement with theory. For 40-nm particles, the average agreement between predicted values of S_{crit} and theoretical values was -2.6% ($1\sigma = 16\%$, $n = 9$) for the model of Weingartner et al. and -1.1% ($1\sigma = 10\%$, $n = 9$) for the model of this work. Results for 100-nm particles were similar. The model of Weingartner et al. performs most poorly for solution droplets formed on particles composed of NH_4NO_3 , H_2SO_4 , and internally mixed $(\text{NH}_4)_2\text{SO}_4$ – NH_4NO_3 . Errors in S_{crit} were between 18% and 26% for these compounds. The osmotic coefficient varies more strongly with RH for NH_4NO_3 and H_2SO_4 , and exhibits a value far from unity (≈ 0.6) for NH_4NO_3 , H_2SO_4 , and $(\text{NH}_4)_2\text{SO}_4$ – NH_4NO_3 over the RH range typical of HTDMA experiments. The other compounds studied

here exhibit osmotic coefficient values that are closer to unity and do not vary as much as those for solutions containing NH_4NO_3 and $(\text{NH}_4)_2\text{SO}_4\text{-NH}_4\text{NO}_3$. Therefore, the simpler model of Weingartner et al. is a reasonable approach for solutions with osmotic coefficients that do not vary significantly over the range of RHs for HTDMA studies and that are not significantly different from the value of Φ for solution droplets at their critical size (at S_{crit}). This model would predict less accurate values of S_{crit} for droplet solutions of unknown chemical composition where the above conditions may not exist. Although the model proposed in this work also has limitations, the inclusion of an additional adjustable parameter expands its range of applicability.

7. Conclusions

A technique for using hygroscopic growth measurements at RHs below 100% to derive the critical supersaturation required to activate a particle to a cloud droplet has been described. A modified Köhler model is derived, including a parameterization for the solution osmotic coefficient that approaches the correct thermodynamic limit as the solution becomes more dilute. The method involves fitting the proposed Köhler model to $(D_{\text{drop}}, \text{RH})$ data pairs obtained from HTDMA studies on a single dry particle size. Chemical composition-dependent unknowns, Y_f and $\beta_{0,f}$, derived from the fit procedure are used to calculate S_{crit} . The various assumptions made in the modified Köhler model, volume additivity, solution surface tension set equal to the surface tension of pure water, and a simplified parameterization for Φ , were independently tested for the range of RH values experienced in the HTDMA by comparing values of x_s , Φ , a_w , the Kelvin term, and RH from the modified and reference models. These comparisons showed that the errors in RH values calculated from the modified model were similar to uncertainties in the reference model values themselves and to typical errors in experimental RH for NaCl, NH_4NO_3 , $(\text{NH}_4)_2\text{SO}_4$, and several internally mixed particle compositions. For NH_4HSO_4 , the RH values from the reference and modified models did not agree as well because the neglected terms in Φ are important for this compound and the full Pitzer model itself does not accurately reproduce the behavior of Φ for NH_4HSO_4 at higher solution molalities (Kim et al. 1993). The proposed parameterization for Φ was also tested for particles composed of H_2SO_4 . It was found that the parameterization could not accurately reproduce the variation of Φ with m for aqueous solutions containing H_2SO_4 .

The technique was studied numerically in order to validate that S_{crit} could be derived within experimental uncertainties. The sensitivity of the predicted values of S_{crit} to assumed uncertainties in the input parameters was investigated as a function of dry particle chemical composition and size. The method is effective at predicting values of S_{crit} for 4- and 100-nm-diameter particles com-

posed of NaCl, $(\text{NH}_4)_2\text{SO}_4$, NH_4HSO_4 , H_2SO_4 , NH_4NO_3 , and for the internally mixed compositions examined. Comparisons between values of S_{crit} predicted by the Köhler model proposed in this work and the simpler model proposed by Weingartner et al. (1997) indicated that both models produced results that agreed well with theoretical values of S_{crit} , except for compounds where the osmotic coefficient varied significantly from its value at S_{crit} . In those cases, the model proposed in this work predicted S_{crit} more accurately. Numerical sensitivity studies showed that values of S_{crit} can be predicted within $-7.5\% \pm 10\%$ using the proposed technique, similar to observed experimental uncertainties in S_{crit} determined from laboratory CCN studies discussed in Part II (Brechtel and Kreidenweis 2000).

Acknowledgments. This work was sponsored by the Environmental Protection Agency under STAR Graduate Fellowship U-914726-01-0. The comments of J. Hudson and an anonymous reviewer are greatly appreciated.

REFERENCES

- Atkins, P. W., 1994: *Physical Chemistry*. Oxford University Press, 1031 pp.
- Berg, O. H., E. Swietlicki, and R. Krejci, 1998: Hygroscopic growth of aerosol particles in the marine boundary layer over the Pacific and Southern Oceans during ACE I. *J. Geophys. Res.*, **103**, 16 535–16 545.
- Brechtel, F. J., 1998: Predicting particle critical supersaturation from hygroscopic growth measurements in the humidified tandem differential mobility analyzer. Ph.D. thesis, Department of Atmospheric Science, Colorado State University, Fort Collins, CO, 267 pp. [Available from Dept. of Atmospheric Science, Colorado State University, Fort Collins, CO 80523.]
- , and S. M. Kreidenweis, 2000: Predicting particle critical supersaturation from hygroscopic growth measurements in the humidified TDMA. Part II: Laboratory and ambient studies. *J. Atmos. Sci.*, **57**, 1872–1887.
- Chen, J.-P., 1994: Theory of deliquescence and modified Köhler curves. *J. Atmos. Sci.*, **51**, 3505–3516.
- Clegg, S. L., and K. S. Pitzer, 1992: Thermodynamics of multicomponent, miscible, ionic solutions: Generalized equations for symmetrical electrolytes. *J. Phys. Chem.*, **96**, 3513–3520.
- Covert, D. S., and J. Heintzenberg, 1984: Measurement of the degree of internal/external mixing of hygroscopic compounds and soot in atmospheric aerosols. *Sci. Total Environ.*, **36**, 347–352.
- , and —, 1993: Size distributions and chemical properties of aerosol at Ny Alesund, Svalbard. *Atmos. Environ.*, **27A**, 2989–2997.
- , J. L. Gras, A. Wiedensohler, and F. Stratmann, 1998: Comparison of directly measured CCN with CCN modeled from the number-size distribution in the MBL during ACE-I at Cape Grim. *J. Geophys. Res.*, **103**, 16 597–16 608.
- Cruz, C. N., and S. N. Pandis, 1997: A study of the ability of pure secondary organic aerosol to act as cloud condensation nuclei. *Atmos. Environ.*, **31**, 2205–2214.
- Fitzgerald, J. W., W. A. Hoppel, and M. A. Vietti, 1982: The size and scattering coefficient of urban aerosol particles at Washington, D.C. as a function of relative humidity. *J. Atmos. Sci.*, **39**, 1838–1852.
- Hallberg, A., J. A. Ogren, K. J. Noone, K. Okada, J. Heintzenberg, and I. B. Svenningsson, 1994: The influence of aerosol particle

- composition on cloud droplet formation. *J. Atmos. Chem.*, **19**, 153–171.
- Hänel, G., 1976: The properties of atmospheric aerosol particles as functions of the relative humidity at thermodynamic equilibrium with the surrounding moist air. *Rev. Geophys.*, **17**, 73–188.
- Hudson, J. G., and X. Da, 1996: Volatility and size of cloud condensation nuclei. *J. Geophys. Res.*, **101**, 4435–4442.
- IPCC, 1995: Radiative forcing of climate change. *Climate Change 1994*, J. T. Houghton, Ed., Cambridge University Press, 572 pp.
- Juozaitis, A., V. Ulevicius, A. Girgzdys, and K. Willeke, 1993: Differentiation of hydrophobic from hydrophilic submicrometer aerosol particles. *Aerosol Sci. Tech.*, **18**, 202–212.
- Kim, Y. P., J. H. Seinfeld, and P. Saxena, 1993: Atmospheric gas-aerosol equilibrium I. Thermodynamic model. *Aerosol Sci. Tech.*, **19**, 157–181.
- Laaksonen, A., P. Korhonen, M. Kulmala, and R. J. Charlson, 1998: Modification of the Köhler equation to include soluble trace cases and slightly soluble substances. *J. Atmos. Sci.*, **55**, 853–862.
- Liu, B. Y. H., D. Y. H. Pui, K. T. Whitby, D. B. Kittelson, Y. Kousaka, and R. L. McKenzie, 1978: The aerosol mobility chromatograph: A new detector for sulfuric acid aerosols. *Atmos. Environ.*, **12**, 99–104.
- McMurry, P. H., and M. R. Stolzenburg, 1989: On the sensitivity of particle size to relative humidity for Los Angeles aerosols. *Atmos. Environ.*, **23**, 497–507.
- , M. Litchy, P. Huang, X. Cai, B. J. Turpin, W. D. Dick, and A. Hanson, 1996: Elemental composition and morphology of individual particles separated by size and hygroscopicity with the TDMA. *Atmos. Environ.*, **30**, 101–108.
- Pitchford, M. L., and P. H. McMurry, 1994: Relationship between measured water vapor growth and chemistry of atmospheric aerosol for Grand Canyon, Arizona, in winter 1990. *Atmos. Environ.*, **28**, 827–839.
- Pitzer, K. S., 1973: Thermodynamics of electrolytes. I. Theoretical basis and general equations. *J. Phys. Chem.*, **77**, 268–277.
- , 1979: Theory: Ion Interaction Approach. *Activity Coefficients of Electrolyte Solutions*, R. M. Pytkowicz, Ed., Vol. 1, CRC Press, 157–208.
- , and G. Mayorga, 1973: Thermodynamics of electrolytes. II. Activity and osmotic coefficients for strong electrolytes with one or both ions univalent. *J. Phys. Chem.*, **77**, 2300–2308.
- Pruppacher, H. R., and J. Klett, 1997: *Microphysics of Clouds and Precipitation*. 2d ed. Dordrecht Publishers, 954 pp.
- Rader, D. J., and P. H. McMurry, 1986: Application of the tandem differential mobility analyzer to studies of droplet growth or evaporation. *J. Aerosol Sci.*, **17**, 771–787.
- Robinson, R. A., and R. H. Stokes, 1959: *Electrolyte Solutions*. 2d ed. Butterworths, 571 pp.
- Rogers, R. R., and M. K. Yau, 1989: *A Short Course in Cloud Physics*. 3d ed. Pergamon Press, 293 pp.
- Rogge, W. F., M. A. Mazurek, L. M. Hildemann, G. R. Cass, and B. R. T. Simoneit, 1993: Quantification of urban organic aerosols at a molecular level: Identification, abundance and seasonal variation. *Atmos. Environ.*, **27A**, 1309–1330.
- Saxena, P., and L. M. Hildemann, 1996: Water-soluble organics in atmospheric particles: A critical review of the literature and application to thermodynamics to identify candidate compounds. *J. Atmos. Chem.*, **24**, 57–109.
- , —, P. H. McMurry, and J. H. Seinfeld, 1995: Organics alter hygroscopic behavior of atmospheric particles. *J. Geophys. Res.*, **100**, 18 755–18 770.
- Schulmann, M. L., M. C. Jacobsen, R. J. Charlson, R. E. Synovec, and T. E. Young, 1996: Dissolution behavior and surface tension effects of organic compounds in nucleating cloud droplets. *Geophys. Res. Lett.*, **23**, 277–280.
- Seinfeld, J. H., 1986: *Atmospheric Chemistry and Physics of Air Pollution*. J. Wiley and Sons, 738 pp.
- Sekigawa, K., 1983: Estimation of the volume fraction of water soluble material in submicron aerosols in the atmosphere. *J. Meteor. Soc. Japan*, **61**, 359–367.
- Stokes, R. H., and R. A. Robinson, 1966: Interactions in aqueous nonelectrolyte solutions. *J. Phys. Chem.*, **70**, 2126–2131.
- Svenningsson, I. B., H.-C. Hansson, A. Wiedensohler, J. A. Ogren, K. J. Noone, and A. Hallberg, 1992: Hygroscopic growth of aerosol particles in the Po Valley. *Tellus*, **44B**, 556–569.
- , —, —, K. Noone, J. Ogren, A. Hallberg, and R. Colville, 1994: Hygroscopic growth of aerosol particles and its influence on nucleation scavenging in cloud: Experimental results from Kleiner Feldberg. *J. Atmos. Chem.*, **19**, 129–152.
- Tang, I. N., 1997: Thermodynamic and optical properties of mixed-salt aerosols of atmospheric importance. *J. Geophys. Res.*, **102**, 1883–1893.
- , and H. R. Munkelwitz, 1994: Water activities, densities, and refractive indices of aqueous sulfates and sodium nitrate droplets or atmospheric importance. *J. Geophys. Res.*, **99**, 18 801–18 808.
- , W. T. Wong, and H. R. Munkelwitz, 1981: The relative importance of atmospheric sulfates and nitrates in visibility reduction. *Atmos. Environ.*, **15**, 2463–2471.
- Weast, R. C., 1988: *Handbook of Chemistry and Physics*. 69th ed. CRC Press, 2348 pp.
- Weingartner, E., H. Burtscher, and U. Baltensperger, 1997: Hygroscopic properties of carbon and diesel soot particles. *Atmos. Environ.*, **31**, 2311–2327.
- Yum, S. S., J. G. Hudson, and Y. Xie, 1998: Comparisons of cloud microphysics with cloud condensation nuclei spectra over the summertime Southern Ocean. *J. Geophys. Res.*, **103**, 16 625–16 636.
- Zhang, X. Q., P. H. McMurry, S. V. Hering, and G. S. Casuccio, 1993: Mixing characteristics and water content of submicron aerosols measured in Los Angeles and at the Grand Canyon. *Atmos. Environ.*, **27A**, 1593–1607.